

Stability Analysis of Convection in the Intracluster Medium

H. Gupta^{a,*}, S.K. Rathor^a, M.E. Pessah^b, S. Chakraborty^{a,c}

^aDepartment of Physics, Indian Institute of Technology Kanpur, U. P.-208016, India

^bNiels Bohr International Academy, Niels Bohr Institute, 2100, Copenhagen Ø, Denmark

^cMechanics & Applied Mathematics Group, Indian Institute of Technology Kanpur, U.P.-208016, India

Abstract

We use the machinery usually employed for studying the onset of Rayleigh–Bénard convection in hydro- and magnetohydrodynamic settings to address the onset of convection induced by the magnetothermal instability and the heat-flux-buoyancy-driven instability in the weakly-collisional magnetized plasma permeating the intracluster medium. Since most of the related numerical simulations consider the plasma being bounded between two ‘plates’ on which boundary conditions are specified, our strategy provides a framework that could enable a more direct connection between analytical and numerical studies. We derive the conditions for the onset of these instabilities considering the effects of induced magnetic tension resulting from a finite plasma beta. We provide expressions for the Rayleigh number in terms of the wave vector associated with a given mode, which allow us to characterize the modes that are first to become unstable. For both the heat-flux-buoyancy-driven instability and the magnetothermal instability, oscillatory marginal stable states are possible.

PACS numbers 98.65.Hb, 44.25.+f

Keywords: Convection, Intracluster medium, Galaxy cluster, Linear stability analysis, Magnetothermal instability, Heat-flux-driven buoyancy instability

1. Introduction

Convection, i.e., the motions induced within a fluid by the tendency of hotter, less dense material to rise, and colder, denser material to sink under the influence of gravity, is a ubiquitous phenomenon in nature. These motions, and the ensuing transfer of heat, can have important implications for a wide variety of systems, see e.g., [Getling \(1997\)](#), ranging from laboratory settings to the Earth and the oceans, from planetary to stellar atmospheres, and from accretion disks ([Stone and Balbus, 1996](#); [Lesur and Ogilvie, 2010](#); [Bodo et al., 2012](#); [Oliver, 2013](#)) to the intracluster medium (ICM) permeating galaxy clusters ([Balbus, 2001](#); [Quataert, 2008](#); [Parrish et al., 2009](#); [Bogdanović et al., 2009](#); [McCourt et al., 2011](#); [Kunz et al., 2012](#)).

The inherent nonlinearity of the governing equations, together with the complex dynamical boundaries present in nature, has motivated the study of convection in idealized settings where the fluid is confined between two parallel horizontal plates and is heated from below. When this setup leads to convective motions, this is termed Rayleigh–Bénard convection (RBC). The stability of the equilibrium state and the flow dynamics in RBC are determined by a non-dimensional parameter viz., the Rayleigh number R , which is a measure of the

strength of the destabilizing buoyancy force relative to the stabilising viscous force in the fluid. When the Rayleigh number for a given fluid is below a critical number, then heat transfer occurs primarily via conduction; when this critical number is exceeded, heat transfer is primarily via convection. The onset of the instability and the critical value of R can be understood by means of a linear stability analysis ([Chandrasekhar, 1981](#)).

The rich nonlinear phenomena (e.g., pattern formation, route to chaos, turbulence, etc.) ensuing in such a convective system can also be analytically investigated in the weakly nonlinear limit ([Bhattacharjee, 1989](#); [Cross and Greenside, 2009](#)). There is a large body of literature on flow reversals, pattern formation and evolution in RBC encompassing both experiments ([Morris et al., 1993](#); [Assenheimer and Steinberg, 1996](#)) as well as nonlinear two-dimensional (2D) ([Chandra and Verma, 2013](#)) and three dimensional (3D) simulations ([Getling and Brausch, 2003](#)).

The study of RBC has benefited the understanding of convection in a wide variety of systems in nature, for instance, in the Earth’s outer core ([Cardin and Olson, 1994](#)), mantle ([Mckenzie, Roberts, and Weiss, 1974](#)), atmosphere ([Hartmann, Moy, and Fu, 2001](#)), and oceans ([Marshall and Schott, 1999](#)), as well as in Sun spots ([Cattaneo, Emonet, and Weiss, 2003](#)), and in metal production processes ([Brent, Voller, and Reid, 1988](#)). The framework employed to study RBC has been generalized by considering the presence of magnetic fields and even incorporating the effects of rotation, a combination prevalent in astrophysical fluids. This approach has shed light into the gener-

*Corresponding author

Email addresses: hiugupta@iitk.ac.in (H. Gupta), skrathor@iitk.ac.in (S.K. Rathor), mpessah@nbi.dk (M.E. Pessah), sagarc@iitk.ac.in (S. Chakraborty)

ation and reversal of the Earth magnetic field (Glatzmaiers and Roberts, 1995) and the internal dynamics of the Sun (Brandenburg et al., 1996; Cattaneo et al., 2003).

In all of the cases in which conducting media have been considered, the plasma has been assumed to behave as a magnetized fluid, as described in the magnetohydrodynamic (MHD) approximation. There are situations of astrophysical interest, however, in which the plasma is only weakly-collisional, i.e., the mean free path for particles to interact is much larger than the Larmor radius. This is the case for the dilute ICM permeating galaxy clusters, in which transport properties are anisotropic with respect to the direction of the magnetic field.

The aim of this letter is to build upon the machinery employed to study RBC in hydro- and magnetohydro-dynamic scenarios in order to address the onset of convection in the weakly-collisional magnetized plasma in galaxy clusters.

1.1. Instabilities in the Weakly-Collisional ICM

The ICM is a weakly collisional and high-beta plasma (see e.g., (Carilli and Taylor, 2002; Peterson and Fabian, 2006)), in which the transport of heat, transport of momentum and diffusion of ions is anisotropic due to the presence of magnetic field. Linear stability analysis has shown that the ICM is dynamically unstable, to the so-called magnetothermal instability, MTI, (Balbus, 2000, 2001) and the heat-flux-driven buoyancy instability, HBI (Quataert, 2008). The MTI sets in when the temperature gradient decreases outwards and the magnetic field lines are perpendicular to the direction of gravity, whereas the HBI is excited when the temperature gradient increases outwards and the magnetic field lines are parallel to the gravitational field. The original studies of these instabilities have been generalized to explore the effects of viscous anisotropy (Ren et al., 2010; Kunz, 2011) and semi-global settings (Latter and Kunz, 2012). More recently, Pessah and Chakraborty (2013); Berlok and Pessah (2015) analyzed the stability of the ICM generalizing previous work by considering the effects of concentration gradients that could be present in the ICM if the sedimentation of Helium is effective (Chuzhoy and Loeb, 2004; Peng and Nagai, 2009; Shtykovskiy and Gilfanov, 2010).

Researchers have carried out nonlinear numerical studies of the MTI (Parrish and Stone, 2005, 2007; Parrish et al., 2008; McCourt et al., 2011) and the HBI (Parrish and Quataert, 2008; Parrish et al., 2009, 2010; McCourt et al., 2011; Kunz et al., 2012) in connection with the ‘cooling flow problem’ in cool core galaxy clusters. The effects of shear flow (and thus, Kelvin-Helmholtz instability) on the stability condition for MTI is explored in Ren et al. (2011). Recently, Nipoti and Posti (2014) performed linear stability analysis on weakly magnetized, rotating plasma in both collisional and collisionless environments, leading to more complete picture of ICM.

1.2. Advantages of the Rayleigh–Bénard Approach

There are a number of advantages that follow from employing the machinery developed for RBC to the study of the MTI and HBI. This approach allows us to shed light into many aspects of the MTI and the HBI, which are thought to play a role in the dynamics of the intracluster medium (ICM). For instance,

1. This framework provides a good platform to several connections with numerical simulations because the boundary conditions (BCs) usually adopted resemble the ones employed in RBC.
2. The results obtained can help us identify the critical Rayleigh number for the onset of the MTI and the HBI.
3. The formalism allows us to account for the effects of magnetic tension on the stability criterion for both the MTI and the HBI. This approach could be useful in order to assess the effects of magnetic tension on the unstable growing modes found to feed off composition gradients in a inhomogeneous intracluster medium (Pessah and Chakraborty, 2013; Berlok and Pessah, 2015)
4. The analysis could enable a low dimensional model like the Lorenz model for RBC (Lorenz, 1963; Chen and Price, 2006) and magnetic RBC (Zierep, 2003), which could give further insights into the chaotic (turbulent) state of the ICM.

2. The Rayleigh–Bénard Framework

Let us consider a weakly-collisional plasma at rest confined between two horizontal parallel plates of infinite extent, as it is shown in Fig. 1. The vertical separation between the plates is d and the acceleration due to gravity \mathbf{g} is acting vertically downwards. The bottom and the top boundaries are held at two different constant temperatures T_{bottom} and T_{top} , respectively. This sets up a constant background temperature gradient in the confined plasma. There is also an externally imposed uniform magnetic field \mathbf{B} lying on the $x - z$ plane and acting on the system under study.

2.1. Governing Equations

The equations of motion describing the dynamics of this system are given by

$$\frac{\partial \rho}{\partial t} + \nabla \cdot (\rho \mathbf{v}) = 0, \quad (1)$$

$$\frac{d\mathbf{v}}{dt} = -\frac{1}{\rho} \nabla \cdot \left(\mathbf{P} + \frac{\mathbf{B}^2}{8\pi} \mathbf{I} - \frac{B^2}{4\pi} \hat{\mathbf{b}}\hat{\mathbf{b}} \right) + \mathbf{g}, \quad (2)$$

$$\frac{\partial \mathbf{B}}{\partial t} = \nabla \times (\mathbf{v} \times \mathbf{B}) + \eta \nabla^2 \mathbf{B}, \quad (3)$$

$$\rho T \frac{ds}{dt} = (p_{\perp} - p_{\parallel}) \frac{d}{dt} \ln \frac{B}{\rho^{\gamma-1}} - \nabla \cdot \mathbf{Q}_s. \quad (4)$$

Here, the Lagrangian and Eulerian derivatives are related via $d/dt \equiv \partial/\partial t + \mathbf{v} \cdot \nabla$, where \mathbf{v} is the fluid velocity. The symbols ρ , T , s , γ and η stand for the fluid density, temperature (assumed to be the same for ions and electrons), specific entropy, adiabatic index and electrical resistivity (also called magnetic diffusivity).

The weakly collisional character of the plasma renders its physical properties anisotropic with respect to the local direction of the magnetic field. The pressure tensor is $\mathbf{P} \equiv p_{\perp} \mathbf{I} + (p_{\parallel} - p_{\perp}) \hat{\mathbf{b}}\hat{\mathbf{b}}$, where \mathbf{I} stands for the 3×3 identity matrix. The symbols \perp and \parallel refer respectively to the directions

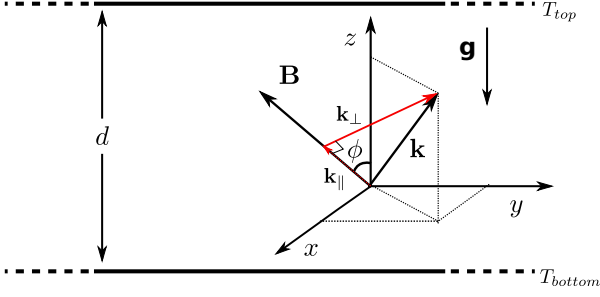


Figure 1: Schematic representation of the model geometry employed to study Rayleigh-Bénard convection (RBC). The dilute, weakly-collisional, magnetized plasma is held between two conducting horizontal plates of infinite extent, separated by a distance d . The plates are maintained at two different constant temperatures as indicated. Gravity is along the negative z axis. The symbols \perp and \parallel represent the directions perpendicular and parallel to the magnetic field, which lies in the $x - z$ plane.

perpendicular and parallel to the magnetic field \mathbf{B} , whose direction is given by the unit vector $\hat{\mathbf{b}} \equiv \mathbf{B}/B = (b_x, 0, b_z)$. If the frequency of ion collisions ν_{ii} in the single ion species magnetofluid is large compared to the rate of change d/dt of all the fields involved, then the anisotropic part of the pressure tensor is small compared to its isotropic part $P \equiv 2p_{\perp}/3 + p_{\parallel}/3$, with $|p_{\parallel} - p_{\perp}| \ll P$. This isotropic part of the pressure tensor is assumed to satisfy the equation of state for an ideal gas

$$P = \frac{\rho k_B T}{\mu m_H}, \quad (5)$$

where k_B is the Boltzmann constant, μ is the mean molecular weight, and m_H is the atomic mass unit. This equation along with Eqs. (1)-(4) completes the specification of the dynamics of the unperturbed equilibrium configuration of the system under study.

The anisotropic component of the pressure tensor in the momentum equation gives rise to Braginskii viscosity. For small pressure anisotropy, this contribution is usually written as

$$p_{\parallel} - p_{\perp} = 3\eta_0 \left(\hat{\mathbf{b}}\hat{\mathbf{b}} - \frac{1}{3}\mathbf{I} \right) : \nabla\mathbf{v}, \quad (6)$$

where η_0 is the largest of the coefficients in the viscous stress tensor derived by Braginskii (1965)[see also Hollweg (1985)], and it is related to the coefficient of kinematic viscosity via $\eta_0 = \rho\nu_v$. This is a good approximation provided that the pressure anisotropy does not grow beyond $|p_{\parallel} - p_{\perp}|/P \approx \beta^{-1}$, where the plasma $\beta \equiv v_{\text{th}}^2/v_A^2$, $v_{\text{th}} \equiv (2P/\rho)^{1/2}$ is the thermal speed, and $v_A \equiv B/(4\pi\rho)^{1/2}$ is the Alfvén speed. The effects of Braginskii viscosity in the linear dynamics of the MTI and the HBI are explored in Kunz (2011). Beyond this limit, various fast-growing, micro-scale plasma instabilities, such as mirror and firehose (see Schekochihin et al. 2005, 2008 and references therein) with growth rates $\gamma \approx k_{\parallel}v_{\text{th}}|p_{\parallel} - p_{\perp}|/P$ can dominate the plasma dynamics at very small scales. Thus, for $|p_{\parallel} - p_{\perp}|/P \gtrsim \beta^{-1}$ the Braginskii-MHD approximation embodied in Eqs. (1)-(4) becomes ill-posed and a mechanism to limit the pressure anisotropy must be implemented in numerical codes (Sharma et al., 2006; Kunz et al., 2012; Parrish et al., 2012).

Dimensional parameters	Symbols	Definitions
Thermal speed of ions	v_{th}	$\sqrt{\frac{2P_i}{\rho_i}}$
Alfvén speed	v_A	$\frac{B}{\sqrt{4\pi\rho_i}}$
Coefficient of thermal expansion	α	$-\frac{1}{\rho} \left(\frac{\partial\rho}{\partial T} \right)_P$
Heat capacity at constant pressure	c_p	$T \left(\frac{ds}{dT} \right)_P$
Coefficient of kinematic viscosity	ν_v	$\frac{\eta_0}{\rho}$
Coefficient of thermal diffusion	λ	$\frac{\chi}{\rho c_p}$
Dimensionless parameters	Symbols	Definitions
Schwarzschild number	S	$\frac{g\alpha T d}{c_p \Delta T} - 1$
Rayleigh number	R	$\frac{\alpha(\Delta T)gd^3}{\lambda\nu_v}$
Chandrasekhar number	Q	$\frac{B^2 d^2}{4\pi\rho\nu_v\eta}$
Prandtl number	P_r	$\frac{\nu_v}{\lambda}$
Magnetic Prandtl number	P_m	$\frac{\nu_v}{\eta}$
Plasma β parameter	β	$\frac{P_i}{B^2/8\pi}$
Knudsen number	Kn	$\frac{\lambda_{\text{mfp}}}{H}$

Table 1: List of parameters used in this letter.

Because the electron mean free path (λ_{mfp}) is large compared to its Larmor radius, heat flows mainly along magnetic field lines. This process is modeled by the second term on the right-hand side of Eq. (4) via $\mathbf{Q}_s \equiv -\chi\hat{\mathbf{b}}(\hat{\mathbf{b}}\cdot\nabla)T$, where χ is the thermal conductivity predominately due to electrons with $\chi \approx 6 \times 10^{-7} T^{5/2} \text{ erg cm}^{-1} \text{ s}^{-1} \text{ K}^{-1}$ (Spitzer, 1962). In the equilibrium state, all the particles in the plasma are assumed to be described by a Maxwellian distribution with the same temperature, so that $p_{\parallel} \equiv p_{\perp}$ initially. In general, the background heat flux does not vanish, i.e., $\hat{\mathbf{b}}\cdot\nabla T \neq 0$, unless the magnetic field and the background gradients are orthogonal. The existence of a well-defined steady state, i.e., $\nabla\cdot\mathbf{Q}_s = 0$, demands that the background heat flux should be at most a linear function of the distance along the direction of the magnetic field.

2.2. Linear Equations for the Perturbations

The equilibrium state $(\rho_*, P_*, T_*, v_*, B_*)$ is defined by the following relations

$$\mathbf{v}_* = 0, \quad (7)$$

$$\frac{dP_*}{dz} \approx \frac{d(p_{\perp})_*}{dz} = -\rho_* g, \quad (8)$$

$$\mathbf{B}_* = B_* \hat{\mathbf{b}} = B_* (\sin\phi\hat{\mathbf{x}} + \cos\phi\hat{\mathbf{z}}), \quad (9)$$

$$T_* = T_{\text{bottom}} - \Delta T \left(\frac{z}{d} \right), \quad (10)$$

where $\Delta T = T_{\text{bottom}} - T_{\text{top}}$, and d is the distance between the top and bottom boundaries. As discussed above, the approximation invoked in Eq. (8) reflects the fact that the pressure anisotropy is relatively weak. We assume that the ion and electron pressures satisfy $P_i = P_e = P/2$ and the ICM to be an ideal gas, and thus

$\alpha T = 1$, where α is the coefficient of thermal expansion. Note that this implies that the Schwarzschild number S , see Table 1, is constant even though T changes with z . Hereafter, we shall drop the asterisk subscripts denoting the equilibrium state as there will be no ambiguity. For the sake of convenience, Table 1 provides a list of all the relevant parameters used in this letter.

Since the sound crossing time associated with the modes of interest is much shorter than the growth rate of the unstable modes of HBI and MTI, it is justified to work within the Boussinesq approximation (Balbus, 2000, 2001; Quataert, 2008). In this limit, Eq. (1) reduces to

$$\nabla \cdot \mathbf{v} = 0. \quad (11)$$

Thus, under the Boussinesq approximation, the velocity field perturbation satisfy $\nabla \cdot \delta \mathbf{v} = 0$. Also, in this approximation the density variations can be ignored except when it appears multiplied with the external gravity term.

Together with the solenoidal character of the magnetic field fluctuations, $\nabla \cdot \delta \mathbf{B} = 0$; the relation $\nabla \cdot \delta \mathbf{v} = 0$ implies that it is only necessary to understand the dynamics of two independent components for both the velocity and the magnetic field components. It is convenient to use as variables $\delta v_z, \delta \omega_z, \delta B_z$, and δj_z , where

$$\delta \omega_z \equiv \partial_x \delta v_y - \partial_y \delta v_x, \quad (12)$$

$$\delta j_z \equiv \partial_x \delta B_y - \partial_y \delta B_x, \quad (13)$$

stand for the z -component of the fluctuations in the vorticity and the current density (times 4π), respectively.

Taking the Laplacian of the z -component of the momentum Eq. (2) and the z -component of its curl, we arrive to the equations of motion for δv_z and $\delta \omega_z$

$$\begin{aligned} \partial_t \nabla^2 \delta v_z &= \alpha g (\partial_x^2 + \partial_y^2) \delta T + \\ &\frac{B}{4\pi\rho} (\sin\phi \partial_x + \cos\phi \partial_z) \nabla^2 \delta B_z \\ &- 3v_\nu (\sin\phi \partial_x + \cos\phi \partial_z)^2 [\cos\phi (\partial_x^2 + \partial_y^2) - \sin\phi \partial_x \partial_z] \\ &\times (\sin\phi \delta v_x + \cos\phi \delta v_z), \end{aligned} \quad (14)$$

$$\begin{aligned} \partial_t \delta \omega_z &= \frac{B}{4\pi\rho} (\sin\phi \partial_x + \cos\phi \partial_z) \delta j_z \\ &+ 3v_\nu \sin\phi \partial_y (\sin\phi \partial_x + \cos\phi \partial_z)^2 (\sin\phi \delta v_x + \cos\phi \delta v_z). \end{aligned} \quad (15)$$

Following a similar procedure with the induction Eq. (3), we obtain the equations for δB_z and δj_z

$$(\partial_t - \eta \nabla^2) \delta B_z = B (\sin\phi \partial_x + \cos\phi \partial_z) \delta v_z, \quad (16)$$

$$(\partial_t - \eta \nabla^2) \delta j_z = B (\sin\phi \partial_x + \cos\phi \partial_z) \delta \omega_z. \quad (17)$$

We obtain the equation for the thermal fluctuations directly

from Eq. (4) as

$$\begin{aligned} \partial_t \delta T + \delta v_z \left(\frac{dT}{dz} + \frac{g\alpha T}{c_p} \right) &= \\ \lambda (\sin^2\phi \partial_x^2 + 2\sin\phi \cos\phi \partial_x \partial_z + \cos^2\phi \partial_z^2) \delta T &+ \\ \frac{\lambda}{B} \frac{dT}{dz} (A_1 \partial_y \delta B_y + A_2 \partial_x \delta B_x + A_3 \partial_z \delta B_z) &+ \\ \frac{\lambda}{B} \frac{dT}{dz} (A_4 \partial_x \delta B_z + A_5 \partial_z \delta B_x), & \end{aligned} \quad (18)$$

where we have defined a number of functions in order to simplify the notation

$$A_1 \equiv \cos\phi, \quad (19)$$

$$A_2 \equiv \cos\phi (\cos^2\phi - \sin^2\phi), \quad (20)$$

$$A_3 \equiv 2\sin^2\phi \cos\phi, \quad (21)$$

$$A_4 \equiv \sin\phi (\sin^2\phi - \cos^2\phi), \quad (22)$$

$$A_5 \equiv -2\sin\phi \cos^2\phi. \quad (23)$$

2.3. Dimensionless Variables

It is convenient to use the characteristic scales in the problem in order to define a set of dimensionless coordinates according to

$$\mathbf{x}' \equiv \mathbf{x}/d, \quad (24)$$

$$t' \equiv tv_\nu/d^2. \quad (25)$$

where v_ν is the coefficient of kinematic viscosity. This allows us to define a set of dimensionless functions for all the dynamical variables of interest, i.e., $\delta v'_z \equiv \delta v_z d/\lambda$, $\delta \omega'_z \equiv \delta \omega_z d^2/\lambda$, $\delta B'_z \equiv \delta B_z/B$, $\delta j'_z \equiv \delta j_z d/B$, and $\delta \theta' \equiv \delta T/\Delta T$, such that

$$\delta v'_z(\mathbf{x}', t') \equiv \sum_{\mathbf{k}'} \hat{\delta v}'_z(z') \exp(i\mathbf{k}' \cdot \mathbf{x}' + \sigma' t'), \quad (26)$$

$$\delta \omega'_z(\mathbf{x}', t') \equiv \sum_{\mathbf{k}'} \hat{\delta \omega}'_z(z') \exp(i\mathbf{k}' \cdot \mathbf{x}' + \sigma' t'), \quad (27)$$

$$\delta B'_z(\mathbf{x}', t') \equiv \sum_{\mathbf{k}'} \hat{\delta B}'_z(z') \exp(i\mathbf{k}' \cdot \mathbf{x}' + \sigma' t'), \quad (28)$$

$$\delta j'_z(\mathbf{x}', t') \equiv \sum_{\mathbf{k}'} \hat{\delta j}'_z(z') \exp(i\mathbf{k}' \cdot \mathbf{x}' + \sigma' t'), \quad (29)$$

$$\delta \theta'(\mathbf{x}', t') \equiv \sum_{\mathbf{k}'} \hat{\delta \theta}'(z') \exp(i\mathbf{k}' \cdot \mathbf{x}' + \sigma' t'). \quad (30)$$

Here, the hat-symbol ($\hat{}$) denotes the z -dependent Fourier transform amplitudes of the various functions involved, which are assumed to be periodic in the plane perpendicular to z . The dimensionless growth-rate (or frequency) σ' characterizes the dynamics of the perturbation with dimensionless wave vector $\mathbf{k}' = (k'_x, k'_y, 0)$.

The linear nature of the equations for the perturbations allows us to follow the dynamics of each mode independently. For the sake of brevity, in what follows, unless otherwise specified, we omit all the primes labeling dimensionless coordinates, variables, and functions. We also omit the hat-symbol denoting the Fourier amplitude of a given mode.

Using the previous definitions, the equations for the perturbations in equations (14)–(18), in dimensionless form, read

$$\begin{aligned} & \left[\sigma(\partial_z^2 - k^2) - \frac{3}{k^2}(i \sin\phi k_x + \cos\phi \partial_z)^2 \times \right. \\ & \left. (\cos\phi k^2 + i \sin\phi k_x \partial_z)^2 \right] \delta v_z = -Rk^2 \delta\theta \\ & + Q \frac{P_r}{P_m} (i \sin\phi k_x + \cos\phi \partial_z) (\partial_z^2 - k^2) \delta B_z \\ & + \left[\frac{3i \sin\phi k_y}{k^2} (i \sin\phi k_x + \cos\phi \partial_z)^2 \right. \\ & \left. (\cos\phi k^2 + i \sin\phi k_x \partial_z) \right] \delta \omega_z, \end{aligned} \quad (31)$$

$$\begin{aligned} & \left[\left(\frac{3 \sin^2 \phi k_y^2}{k^2} \right) (i \sin\phi k_x + \cos\phi \partial_z)^2 \right] \delta \omega_z + \sigma \delta \omega_z = \\ & Q \frac{P_r}{P_m} (i \sin\phi k_x + \cos\phi \partial_z) \delta j_z + \left[\frac{3i \sin\phi k_y}{k^2} \times \right. \\ & \left. (i \sin\phi k_x + \cos\phi \partial_z)^2 (\cos\phi k^2 + i \sin\phi k_x \partial_z) \right] \delta v_z, \end{aligned} \quad (32)$$

$$(\partial_z^2 - k^2 - P_m \sigma) \delta B_z = -\frac{P_m}{P_r} (i \sin\phi k_x + \cos\phi \partial_z) \delta v_z, \quad (33)$$

$$(\partial_z^2 - k^2 - P_m \sigma) \delta j_z = -\frac{P_m}{P_r} (i \sin\phi k_x + \cos\phi \partial_z) \delta \omega_z, \quad (34)$$

$$\begin{aligned} & (\cos^2 \phi \partial_z^2 + 2i \sin\phi \cos\phi k_x \partial_z - \sin^2 \phi k_x^2 - P_r \sigma) \delta\theta \\ & = S \delta v_z + \frac{1}{k^2} \left[(A_1 - A_2) k_x k_y + i A_5 k_y \partial_z \right] \delta j_z + \\ & \left[-\frac{A_1}{k^2} k_y^2 \partial_z - \frac{A_2}{k^2} k_x^2 \partial_z + A_3 \partial_z + i A_4 k_x + i \frac{A_5}{k^2} k_x \partial_z^2 \right] \delta B_z. \end{aligned} \quad (35)$$

In writing the preceding set of equations, we have also made use of the following relations:

$$\delta v_x = (ik_x \partial_z \delta v_z + ik_y \delta \omega_z) / k^2, \quad (36)$$

$$\delta v_y = (ik_y \partial_z \delta v_z - ik_x \delta \omega_z) / k^2, \quad (37)$$

$$\delta B_x = (ik_x \partial_z \delta B_z + ik_y \delta j_z) / k^2, \quad (38)$$

$$\delta B_y = (ik_y \partial_z \delta B_z - ik_x \delta j_z) / k^2. \quad (39)$$

2.4. Boundary Conditions

There are several sets of BCs that are commonly adopted in the framework of RBC. In what follows, we shall concern ourselves exclusively with the reflective, stress-free, and perfectly conducting boundaries given by

$$\delta v_z(0) = \delta v_z(1) = 0, \quad (40)$$

$$\partial_z^2 \delta v_z(0) = \partial_z^2 \delta v_z(1) = 0, \quad (41)$$

$$\partial_z \delta \omega_z(0) = \partial_z \delta \omega_z(1) = 0, \quad (42)$$

$$\delta B_z(0) = \delta B_z(1) = 0, \quad (43)$$

$$\partial_z \delta j_z(0) = \partial_z \delta j_z(1) = 0, \quad (44)$$

$$\delta\theta(0) = \delta\theta(1) = 0. \quad (45)$$

Physically, Eq. (40) implies that the normal component of the velocity must be zero on the boundary surfaces, whereas Eqs. (41) and (42) require stress-free surfaces and Eqs. (43) and (44) imply perfectly conducting boundaries. Eq. (45) fixes the boundary surfaces to be at a constant temperature,

For completeness, we state the type of BCs usually adopted in the literature related to the MTI and the HBI. The BC on the velocity is usually reflective, as embodied in Eqs. (40)–(42), see, e.g., [McCourt et al. \(2011\)](#); [Kunz et al. \(2012\)](#). In these papers, the temperature is also fixed at the boundaries as in our Eq. (45). The BCs employed in [Kunz et al. \(2012\)](#) for the magnetic field are $\partial_z \delta B_x = \partial_z \delta B_y = 0$ (Eq. 44) and $\delta B_z = 0$ (Eq. 43) when simulating an initially horizontal field and $\delta B_x = \delta B_y = 0$ and $\partial_z \delta B_z = 0$ when simulating an initially vertical field.

The BCs that we use have the advantage of allowing us to derive analytic solutions. In principle, we could have adopted BCs similar to the ones used in numerical simulations but this would in general require to solve the problem numerically, even in the linear regime. In passing, we may also mention that it is numerically straightforward to impose the BCs chosen in this letter making it possible to have future comparisons with numerical simulations.

2.5. Relevant Characteristic ICM Values

In the analysis that follows, it is of central importance to realize the extreme values that some of the dimensionless parameters in Table 1 can reach under the conditions expected in the ICM. For instance, the dimensionless parameters Q and P_m have extremely large values. In order to set the scale, let us consider as an example ([Carilli and Taylor, 2002](#); [Peterson and Fabian, 2006](#)), e.g., $B \sim 10^{-6} - 10^{-7} \text{G}$, $\rho \sim 10^{-27} - 10^{-25} \text{gm cm}^{-3}$, $\eta = 10 - 10^2 \text{cm}^2 \text{s}^{-1}$, $\nu_v = 10^{25} - 10^{30} \text{cm}^2 \text{s}^{-1}$, $T \sim 10^7 - 10^8 \text{K}$ and radial length $d \sim 10^{24} - 10^{25} \text{cm}$. We thus find $Q \sim 10^{24} - 10^{40}$ and $P_m \sim 10^{23} - 10^{29}$. This result suggests that it is justifiable to work in the limit in which $Q, P_m \rightarrow \infty$. However, as we will show below, some of the results obtained in the stability analysis that follows from the RB approach are sensitive to these limits being taken with the proper care.

3. The Heat-Flux Driven Buoyancy Instability

Let us first consider the case in which the magnetic field is along the z -direction, i.e., $\phi = 0$, which is known to be prone to the HBI ([Quataert, 2008](#)). The RB formalism enables us to find the conditions for the existence of the HBI marginal state as follows.

In the state of marginal stability ($\sigma = 0$), the system of

Eqs. (31)–(32) reduces to

$$3k^2 \partial_z^2 \delta v_z = -Q \frac{P_r}{P_m} \partial_z (\partial_z^2 - k^2) \delta B_z - Rk^2 \delta \theta, \quad (46)$$

$$\partial_z^2 \delta \theta = S \delta v_z - \partial_z \delta B_z, \quad (47)$$

$$(\partial_z^2 - k^2) \delta B_z = -\frac{P_m}{P_r} \partial_z \delta v_z, \quad (48)$$

$$(\partial_z^2 - k^2) \delta j_z = -\frac{P_m}{P_r} \partial_z \delta \omega_z, \quad (49)$$

$$\partial_z \delta j_z = 0, \quad (50)$$

subject to the BCs, $\delta v_z = [3k^2 + Q] \partial_z^2 \delta v_z = \partial_z^2 \delta v_z = 0, \partial_z \delta j_z = 0, \partial_z \delta \omega_z = 0, \delta B_z = 0$ at $z = 0, 1$. Note that δj_z and $\delta \omega_z$ have become decoupled from $\delta v_z, \delta B_z,$ and $\delta \theta$. From Eqs. (49) and (50) and the corresponding boundary conditions, it may be observed that, while the current density's vertical component vanishes identically and the vorticity's vertical component is independent of z at the marginal state we have

$$\delta j_z = 0; \delta \omega_z = \text{constant}. \quad (51)$$

The set of Eqs. (46), (47) and (48) can be combined to give

$$(3k^2 \partial_z^4 - S R k^2) (\partial_z^2 - k^2) \delta v_z = + \left[R \frac{P_m}{P_r} k^2 + Q (\partial_z^2 - k^2) \partial_z^2 \right] \partial_z^2 \delta v_z. \quad (52)$$

In the limit $Q, P_m \rightarrow \infty$ of interest, Eq. (52) reduces to

$$\left[R \frac{P_m}{P_r} k^2 + Q (\partial_z^2 - k^2) \partial_z^2 \right] \partial_z^2 \delta v_z = 0, \quad (53)$$

and also leads to the conclusion that at the boundaries, $z = 0, 1,$

$$\partial_z^4 (\partial_z^2 - k^2) \delta v_z = 0. \quad (54)$$

The most general solution to (53) has the form

$$\delta v_z(z) = C_0 + C_1 z + C_2 \cos k_- z + C_3 \sin k_- z + C_4 \cosh k_+ z + C_5 \sinh k_+ z, \quad (55)$$

where C_0, C_1, C_2, C_3, C_4 and C_5 are constants of integration, and

$$k_+ \equiv \frac{k}{\sqrt{2}} \left[\left(1 + \frac{4|R|P_m}{QP_r k^2} \right)^{1/2} + 1 \right]^{1/2}, \quad (56)$$

$$k_- \equiv \frac{k}{\sqrt{2}} \left[\left(1 + \frac{4|R|P_m}{QP_r k^2} \right)^{1/2} - 1 \right]^{1/2}. \quad (57)$$

Here, we have assumed that the upper boundary is hotter than the bottom one, as discussed below. Therefore, the application of BCs allows us to conclude that $C_0 = C_1 = C_2 = C_4 = C_5 = 0$ and $k_- = n\pi$ ($n \in \mathbb{N}$), giving

$$\delta v_z = C_3 \sin n\pi z, \quad (58)$$

along with

$$R = -n^2 \pi^2 \left[\frac{n^2 \pi^2 + k^2}{k^2} \right] Q \frac{P_r}{P_m}. \quad (59)$$

The marginal state can then exist only if ΔT is negative, i.e., if the upper boundary is hotter. Hence, by setting the temperature difference in the definition of the Rayleigh number R in Eq. (59) to be $-\Delta T$, we obtain

$$\frac{-\alpha(\Delta T)gd^3}{\lambda v_v} = -n^2 \pi^2 \left[\frac{n^2 \pi^2 + k^2}{k^2} \right] Q \frac{P_r}{P_m}, \quad (60)$$

and thus

$$\frac{d \ln T}{dz} = n^2 \pi^2 \left[\frac{n^2 \pi^2 + k^2}{k^2} \right] \left(\frac{1}{\beta H} \right), \quad (61)$$

where we have set $d = H$, with H the thermal-pressure scale height. Note that for a given k , the lowest value of $d \ln T/dz$ occurs when $n = 1$ (*lowest mode*) giving:

$$\frac{d \ln T}{dz} = \pi^2 \left[\frac{\pi^2 + k^2}{k^2} \right] \left(\frac{1}{\beta H} \right). \quad (62)$$

For all $d \ln T/dz$ smaller than this, all the perturbation with wavenumber k are stable and they become unstable as this limit is overcome. Since $d \ln T/dz$, for a given n , is a monotonically decreasing function of k , the minimum or *critical* temperature gradient for the onset of the HBI occurs mathematically at $k = k_c = \infty$. However, it is worth keeping in mind that in order for the fluid approach to remain valid, the wavenumber must satisfy $k \lesssim 2\pi/\lambda_{\text{mfp}}$, or in dimensionless numbers, $k \lesssim 2\pi \text{Kn}^{-1}$. Therefore, using $k = 2\pi \text{Kn}^{-1}$, the critical temperature gradient for the onset of the HBI is obtained as

$$\left. \frac{d \ln T}{dz} \right|_c = \frac{\pi^2 (\text{Kn}^2 + 4)}{4\beta H} \approx \frac{\pi^2}{\beta H}. \quad (63)$$

This threshold for the temperature gradient takes into account the effect of magnetic tension induced by a finite value of the plasma β parameter, which has been usually ignored when deriving the stability criterion for the HBI. In the limit of $\beta \rightarrow \infty$, Eq. (63) recovers the usual criterion for the HBI (Quataert, 2008).

In general, one can use variational principles to investigate the presence of oscillatory marginal states and the validity of the principle of exchange of instabilities (Chandrasekhar, 1981). However, in what follows we show that the lowest mode always appears as a stationary state for the HBI. For this purpose we set $\sigma = iq$, q being real, and rewrite the relevant Eqs. (31), (33), and (35)

$$\left[iq(\partial_z^2 - k^2) - 3k^2 \partial_z^2 \right] \delta v_z = Q \frac{P_r}{P_m} \partial_z (\partial_z^2 - k^2) \delta B_z - Rk^2 \delta \theta, \quad (64)$$

$$(\partial_z^2 - k^2 - iP_m q) \delta B_z = -\frac{P_m}{P_r} \partial_z \delta v_z. \quad (65)$$

$$(\partial_z^2 - iP_r q) \delta \theta = S \delta v_z - \partial_z \delta B_z, \quad (66)$$

In the limit $Q, P_m \rightarrow \infty$ of interest, it is trivial to arrive at the following using the real and imaginary parts of the previous

three equations:

$$\begin{aligned} q^2 P_m [(\partial_z^2 - k^2) \partial_z^2 + 3P_r k^2 \partial_z^2] \delta v_z = \\ -Q(\partial_z^2 - k^2) \partial_z^4 \delta v_z - R \frac{P_m}{P_r} k^2 \partial_z^2 \delta v_z, \end{aligned} \quad (67)$$

$$\begin{aligned} -q P_m [-3k^2 \partial_z^4 + q^2 P_r (\partial_z^2 - k^2) + RS k^2] \delta v_z = \\ q P_r Q (\partial_z^2 - k^2) \partial_z^2 \delta v_z. \end{aligned} \quad (68)$$

Using $\delta v_z = C_3 \sin \pi z$ as the lowest mode for a top-hot-plate configuration and making use of Eqs. (67) and (68), one can arrive at the following relations

$$q^2 P_m [(\pi^2 + k^2) - 3P_r k^2] = Q(\pi^2 + k^2) \pi^2 + R \frac{P_m}{P_r} k^2, \quad (69)$$

and

$$\begin{aligned} q P_m [3k^2 \pi^4 + q^2 P_r (\pi^2 + k^2) - RS k^2] = \\ -q P_r Q (\pi^2 + k^2) \pi^2. \end{aligned} \quad (70)$$

Multiplying (69) by $q P_r$ and adding with (70), we conclude that either $q = 0$ or

$$3q^2 P_r^2 = R(S - 1) - 3\pi^4. \quad (71)$$

For typical values of the parameters in a galaxy cluster, Eq. (71) can be satisfied for all k and for any real q . Therefore the lowest unstable HBI mode can set in as an oscillatory marginal state.

4. The Magnetothermal Instability

When the magnetic field is aligned with the x -direction, and thus it is perpendicular to the direction of gravity, i.e., $\phi = \pi/2$, the plasma may be subject to the MTI (Balbus, 2001). At marginal stability, we can formulate the problem by setting $\sigma = 0$ in Eqs. (31)–(35), which become

$$-\frac{3}{k^2} k_x^4 \partial_z^2 \delta v_z = -Rk^2 \delta \theta + iQ \frac{P_r}{P_m} k_x (\partial_z^2 - k^2) \delta B_z + \frac{3k_x^3 k_y}{k^2} \partial_z \delta \omega_z, \quad (72)$$

$$-\frac{3k_x^2 k_y^2}{k^2} \delta \omega_z = \frac{3k_x^3 k_y}{k^2} \partial_z \delta v_z + iQ \frac{P_r}{P_m} k_x \delta j_z, \quad (73)$$

$$(\partial_z^2 - k^2) \delta B_z = -i \frac{P_m}{P_r} k_x \delta v_z, \quad (74)$$

$$(\partial_z^2 - k^2) \delta j_z = -i \frac{P_m}{P_r} k_x \delta \omega_z, \quad (75)$$

$$-k_x^2 \delta \theta = S \delta v_z + ik_x \delta B_z, \quad (76)$$

subject to the BCs, at $z = 0, 1$,

$$\begin{aligned} \delta \theta = 0; \quad \delta v_z = \partial_z^2 \delta v_z = 0; \\ \partial_z \delta j_z = 0; \quad \partial_z \delta \omega_z = 0; \quad \delta B_z = 0. \end{aligned} \quad (77)$$

One can see that the BC for the temperature $\delta \theta$ is trivially satisfied due to the BCs on δv_z and δB_z . Combining Eqs. (72)–(73),

we get the following differential equation for δv_z

$$\begin{aligned} Q \left[RS k^2 k_x^2 (\partial_z^2 - k^2) + \frac{3}{k^2} k_x^8 \partial_z^2 (\partial_z^2 - k^2) + \frac{3}{k^2} k_x^6 k_y^2 (\partial_z^2 - k^2)^2 \right] \delta v_z \\ + Q^2 k_x^6 (\partial_z^2 - k^2) \delta v_z + QR \frac{P_m}{P_r} k^2 k_x^4 \delta v_z + 3RS k_x^2 k_y^2 (\partial_z^2 - k^2)^2 \delta v_z \\ + 3Rk_x^4 k_y^2 \frac{P_m}{P_r} (\partial_z^2 - k^2) \delta v_z = 0. \end{aligned} \quad (78)$$

We focus on the limit of interest, i.e., $Q, P_m \rightarrow \infty$, which in this case allows us to write the following single differential equation for δv_z , where it is only necessary to retain terms up to order Q^2 , P_m^2 and QP_m have been kept:

$$Q^2 k_x^6 (\partial_z^2 - k^2) \delta v_z + QR \frac{P_m}{P_r} k^2 k_x^4 \delta v_z = 0. \quad (79)$$

Taking the successive even z -derivatives of this equation and evaluating the results at $z = 0, 1$ we obtain

$$\partial_z^{2m} \delta v_z = 0 \quad \text{with} \quad m \in \{0, 1, 2, \dots\}. \quad (80)$$

This means that the appropriate solution for the lowest mode is

$$\delta v_z = A \sin \pi z, \quad (81)$$

where A is a constant. Therefore, Eq. (79) implies:

$$R = \frac{k_x^2}{k^2} (\pi^2 + k^2) Q \frac{P_r}{P_m}, \quad (82)$$

where $k_x \neq 0$. The marginal state can exist only if ΔT is positive, i.e., if the bottom boundary is hotter. Note that for fixed k_x , the Rayleigh number R monotonically decreases as k_y increases; and, for fixed k_y , R monotonically increases with k_x . Also, recall that in order for the local analysis in (x, y) to be valid within the fluid approach we should have $H^{-1} < k_x, k_y < \lambda_{\text{mfp}}^{-1}$. Therefore, we note that, while the minimum possible value of k_x is $(k_x)_{\text{min}} \gtrsim 2\pi$, the maximum value of k_y is $(k_y)_{\text{max}} \lesssim 2\pi/\text{Kn}$ and this combination (k_x, k_y) corresponds to the lowest unstable mode.

The minimum value for the temperature gradient $-d \ln T/dz$ for the onset of MTI modes with $k_x, k_y \neq 0$, is obtained from

$$-\frac{d \ln T}{dz} \Big|_c = \min \left[\frac{k_x^2 (\pi^2 + k_x^2 + k_y^2)}{k_x^2 + k_y^2} \right] \left(\frac{1}{\beta H} \right), \quad (83)$$

where the minimum value

$$\begin{aligned} \min \left[\frac{k_x^2 (\pi^2 + k_x^2 + k_y^2)}{k_x^2 + k_y^2} \right] \equiv \\ \frac{(k_x)_{\text{min}}^2 [\pi^2 + (k_x)_{\text{min}}^2 + (k_y)_{\text{max}}^2]}{(k_x)_{\text{min}}^2 + (k_y)_{\text{max}}^2}, \end{aligned} \quad (84)$$

depends on the particular mode under consideration. This threshold for the temperature gradient takes into account the effect of magnetic tension induced by a finite value of the plasma β parameter, which has been usually ignored when deriving the stability criterion for the MTI. In the limit of $\beta \rightarrow \infty$, Eq. (83) recovers the usual criterion for the MTI (Balbus, 2001).

We now show that the lowest mode doesn't set in as an oscillatory marginal stability state. In order to achieve this, let us define $\sigma = iq$, with q real and write the relevant version of Eqs. (31)–(35) as

$$\left[iq(\partial_z^2 - k^2) - \frac{3k_x^3 k_y}{k^2} \partial_z \delta \omega_z \right] \delta v_z = iQ \frac{P_r}{P_m} k_x (\partial_z^2 - k^2) \delta B_z - Rk^2 \delta \theta + \frac{3k_x^3 k_y}{k^2} \partial_z \delta \omega_z, \quad (85)$$

$$\left(-\frac{3k_x^2 k_y^2}{k^2} - iq \right) \delta \omega_z = \frac{3k_x^3 k_y}{k^2} \partial_z \delta v_z + iQ \frac{P_r}{P_m} k_x \delta j_z. \quad (86)$$

$$(\partial_z^2 - k^2 - iP_m q) \delta B_z = -i \frac{P_m}{P_r} k_x \delta v_z, \quad (87)$$

$$(\partial_z^2 - k^2 - iP_m q) \delta j_z = -i \frac{P_m}{P_r} k_x \delta \omega_z, \quad (88)$$

In the limit $Q, P_m \rightarrow \infty$, one can as before argue in favour of using $\delta v_z = A \sin \pi z$ as the lowest mode. Using the immediately preceding five equations, it is easy to arrive at the following real and imaginary parts of a complex equation, leading to

$$q^4 \left[(\pi^2 + k^2) \left(k_x^2 + \frac{k_x^2 k_y^2}{k^2} P_r \right) - \frac{3k_x^4}{k^2} P_r \pi^2 \right] + q^2 \left[\frac{Rk_x^2 k^2}{P_r} + 3RSk_x^2 k_y^2 \right] - q^2 \left[\frac{Qk_x^2}{P_m} \left(k_x^2 - \frac{3k_x^2 k_y^2}{k^2} P_r \right) (\pi^2 + k^2) \right] = 0, \quad (89)$$

$$q^5 P_r (\pi^2 + k^2) + q^3 \left[\frac{3k_x^6}{k^2} \pi^2 + \frac{3k_x^4 k_y^2}{k^2} (\pi^2 + k^2) \right] - q^3 \left[RSk^2 + \frac{QP_r}{P_m} k_x^2 (\pi^2 + k^2) \right] - q \left[\left(\frac{Q}{P_m} \right) \frac{3k_x^6 k_y^2}{k^2} (\pi^2 + k^2) - \frac{3k_x^4 k_y^2}{P_r} R \right] = 0. \quad (90)$$

In the light of Eq. (82), these two equations simplify respectively to

$$q^4 \left[(\pi^2 + k^2) \left(k_x^2 + \frac{k_x^2 k_y^2}{k^2} P_r \right) - \frac{3k_x^4}{k^2} P_r \pi^2 \right] + q^2 \left[3R(S+1)k_x^2 k_y^2 \right] = 0, \quad (91)$$

$$q^5 \left[P_r (\pi^2 + k^2) \right] + q^3 \left[\frac{3k_x^6}{k^2} \pi^2 + \frac{3k_x^4 k_y^2}{k^2} (\pi^2 + k^2) - R(S+1)k^2 \right] = 0. \quad (92)$$

Since $\Delta T > 0$ in this case, all the terms inside the square brackets are positive definite allowing us to conclude that for the existence of an oscillatory marginal state $q \neq 0$, we must have

$$\begin{vmatrix} m_{11} & m_{12} \\ m_{21} & m_{22} \end{vmatrix} = 0. \quad (93)$$

where the elements in the determinant are

$$m_{11} = (\pi^2 + k^2) \left(k_x^2 + \frac{k_x^2 k_y^2}{k^2} P_r \right) - \frac{3k_x^4}{k^2} P_r \pi^2, \quad (94)$$

$$m_{12} = 3R(S+1)k_x^2 k_y^2, \quad (95)$$

$$m_{21} = P_r (\pi^2 + k^2), \quad (96)$$

$$m_{22} = \frac{3k_x^6}{k^2} \pi^2 + \frac{3k_x^4 k_y^2 (\pi^2 + k^2)}{k^2} - R(S+1)k^2. \quad (97)$$

While this condition, in principle, allows for the existence of a marginal oscillatory stability state for MTI, it is not easy to explicitly specify analytically the values of k_x and k_y for which this happens. Thus, without solving explicitly this equation in terms of (k_x, k_y) , it is not possible for us to rule out the onset of the MTI as an oscillatory mode.

4.1. Retrieving Schwarzschild Criterion

Before we end this section, it is instructive to note how the limits $Q, P_m \rightarrow \infty$ play an important role to bring about the correct criterion for the onset of the MTI.

Let us consider modes with $k_x \rightarrow 0$, *without necessarily* imposing the limits $Q, P_m \rightarrow \infty$. In this case, using (72)–(73), we arrive at

$$\frac{3k_x^8}{k^2} \mathfrak{D} \partial_z^2 (\partial_z^2 - k^2) \delta v_z + \frac{9k_x^8 k_y^2}{a^4} \partial_z^2 (\partial_z^2 - k^2)^2 \delta v_z = \quad (98)$$

$$Qk_x^6 (\partial_z^2 - k^2) \mathfrak{D} \delta v_z + RSk^2 k_x^2 (\partial_z^2 - k^2) \mathfrak{D} \delta v_z + R \frac{P_m}{P_r} k^2 k_x^4 \mathfrak{D} \delta v_z,$$

where we have introduced, $\mathfrak{D} \equiv Q + 3(k_y^2/k^2)(\partial_z^2 - k^2)$. Hence taking the limit $k_x \rightarrow 0$ yields

$$RSk^2 (\partial_z^2 - k^2) \left[Q + 3 \frac{k_y^2}{k^2} (\partial_z^2 - k^2) \right] \delta v_z = 0. \quad (99)$$

Using $\delta v_z = A \sin \pi z$ as the lowest mode, the condition for marginally stable state is $RS = 0$, i.e.,

$$\Delta T \left[\frac{g\alpha T d}{c_p (\Delta T)} - 1 \right] = 0, \quad (100)$$

and thus

$$-\frac{dT}{dz} = \frac{g\alpha T}{c_p}. \quad (101)$$

This condition, which is independent of the choice of a specific mode for δv_z , is just the condition for the marginal state corresponding to the Schwarzschild instability. Perhaps a more direct way to arrive to this condition is to set $k_x = 0$ in Eq. (76) and assume that $\delta v_z \neq 0$, which leads to the conclusion that the Schwarzschild number is $S = 0$, implying that $-dT/dz = g\alpha T/c_p$, as stated in Eq. (101).

It is not difficult to understand the physics that allow us to retrieve the Schwarzschild instability criterion in the limit $k_x \rightarrow 0$. In an unmagnetized stratified atmosphere, a fluid element that is adiabatically displaced upwards returns to its

initial position if the entropy gradient is positive. This condition is known as Schwarzschild criterion. Now, in the case of the MTI, an upwardly displaced fluid element carries the magnetic field along while retaining its temperature unchanged because the heat quickly flows along the magnetic field lines. This mechanism leads to the MTI. When a perturbation with $k_x \rightarrow 0$ is considered, we could envision the associated mode to have an infinitely long wavelength and thus a fluid parcel displaced upwards is not connected via magnetic field lines to its initial position (i.e., the horizontal layer of atmosphere where it was initially in). Therefore, heat is unable to flow into the displaced layer and one obtains back the Schwarzschild criterion for instability. In this context, it may be noted how setting $k_x = 0$ prevents the magnetic field and the temperature perturbations in Eq. (76) from coupling to the velocity perturbation.

5. Summary and Discussion

In this letter, we have applied the formalism employed in RBC to study the MTI and the HBI. This approach goes beyond the standard linear mode analysis that has been carried out (but see [Latter and Kunz 2012](#) for an exception) by considering explicit boundary conditions. This enabled us to address in a natural way, some aspects of the linear dynamics of these instabilities that have not been previously addressed.

In particular, we have derived the conditions for the onset of the instabilities retaining the effects of magnetic tension, as embodied by a finite plasma beta parameter, and Braginskii viscosity. The latter is known to have a stabilizing effect on the high- k end of the spectrum of unstable modes ([Kunz, 2011](#)). We found, however, that (to linear order) Braginskii viscosity does not play an explicit role in the criterion for the onset of either the HBI or the MTI, see Eqs. (63) and (83). We have found expressions for the Rayleigh number in terms of the wave vector \mathbf{k} of a given mode. In the case of the HBI, the Rayleigh number is found to be a monotonically decreasing function of the mode wavenumber, k . This implies that, for a given temperature gradient, the modes that go unstable first are those with largest values of k , i.e., those with smallest wavelength. In the case of the MTI, the dependence of the Rayleigh number on the dimensionless wave vector \mathbf{k} is more subtle, as it depends on both its magnitude and direction. The MTI modes that go unstable first are those with long wavenumber while maintaining $k_{\parallel} \rightarrow 0$, which is a restriction that does not apply to HBI. For the HBI, the mode that goes unstable first does so in a non-oscillatory fashion, whereas in the MTI, an oscillatory marginal stable state is, in principle, possible.

We have found that the HBI is regularized (at high wavenumbers) by magnetic tension, but such regularization is not present for the MTI. For collisional plasmas, there is a high- k regularization by isotropic viscosity and conductivity. In the weakly-collisional regime that concerns us here, the transport is dominant along magnetic field lines. Nevertheless, there is still some, albeit small, isotropic diffusion. In order to find a critical Rayleigh number for the MTI, as needed to perform a weakly nonlinear analysis, it might be useful to include this isotropic

contribution. While it is certainly possible to include this effect in the equations, this would render the analytical treatment that we have presented significantly more challenging. It is thus pragmatic to defer this calculation to future work while allowing the present work to focus solely on the nontrivial effects of anisotropic heat conduction.

Before we conclude, we comment on the choice of the BCs. For the sake of analytical simplicity, we have chosen to work with conducting stress-free BC. Other possibilities include non-conducting stress-free, conducting rigid, non-conducting rigid, etc. For some of these BCs, it is not possible to solve the problem solely on analytical grounds, and numerical techniques are necessary even in the linear regime. The BC we have employed resemble those usually employed in numerical simulations. The specific choice of boundary conditions is unlikely to have a dramatic impact in the stability criterion within the bulk of the plasma. Nevertheless, it should be kept in mind that these could have an impact on the specific expression for the stability criteria.

Some of these results could have been obtained by other means, for example by retaining the effects of magnetic tension and solving analytically the associated dispersion relations. However, the formalism we have outlined could become even more advantageous as the dispersion relations dictating the linear dynamics become more involved. It is worth noticing that the formalism can be generalized to address more realistic physical settings, for example including the effects of cosmic-rays ([Chandran and Dennis, 2006](#)), rotation ([Nipoti and Posti, 2014](#)), and radiative cooling ([Balbus and Reynolds, 2010](#); [Latter and Kunz, 2012](#)), or composition gradients in the ICM ([Pessah and Chakraborty, 2013](#); [Berlok and Pessah, 2015](#)).

One advantage of having laid out the RBC formalism is that this provides the grounds for future work on weakly-non linear analysis. This type of analysis has proven to be advantageous in delivering further analytical insights into the bifurcation scenarios and the routes to chaotic (turbulent) states of the systems under study ([Bhattacharjee, 1989](#); [Getling, 1997](#)).

Acknowledgments

We are thankful to Thomas Berlok and Mahendra K. Verma for useful discussions. The research leading to these results has received funding from the European Research Council under the European Union's Seventh Framework Programme (FP/2007-2013) under ERC grant agreement 306614 (MEP). MEP also acknowledges support from the Young Investigator Programme of the Villum Foundation (VKR022591). SC gratefully acknowledges the financial support from INSPIRE faculty award (DST/INSPIRE/04/2013/000365) conferred by the Indian National Science Academy (INSA) and the Department of Science and Technology (DST), India.

References

References

Assenheimer, M., Steinberg, V., 1996. Observation of coexisting upflow and downflow hexagons in boussinesq rayleigh-bénard convection. *Phys. Rev.*

- Lett. 76 (5), 756–759.
- Balbus, S. A., 2000. Stability, instability, and "backward" transport in stratified fluids. *Astrophys. J.* 534 (1), 420.
- Balbus, S. A., 2001. Convective and rotational stability of a dilute plasma. *Astrophys. J.* 562 (2), 909.
- Balbus, S. A., Reynolds, C. S., 2010. Radiative and dynamic stability of a dilute plasma. *Astrophys. J. Lett.* 720 (1), L97.
- Berlok, T., Pessah, M. E., 2015. Plasma instabilities in the context of current helium sedimentation models: Dynamical implications for the icm in galaxy clusters. *Astrophys. J.* 813, 22.
- Bhattacharjee, J., 1989. *Convection and Chaos in Fluids*. World Scientific Publishing Co Pte Ltd.
- Bodo, G., Cattaneo, F., Mignone, A., Rossi, P., 2012. Magnetorotational turbulence in stratified shearing boxes with perfect gas equation of state and finite thermal diffusivity. *Astrophys. J.* 761, 116.
- Bogdanović, T., Reynolds, C. S., Balbus, S. A., Parrish, I. J., 2009. Simulations of magnetohydrodynamics instabilities in intracluster medium including anisotropic thermal conduction. *Astrophys. J.* 704, 211–225.
- Braginskii, S. I., 1965. Transport processes in a plasma. *Rev. Plasma Phys.* 1, 205.
- Brandenburg, A., Jennings, R. L., Nordlund, A., Rieutord, M., Stein, R. F., Tuominen, I., 1996. Magnetic structures in a dynamo simulation. *J. Fluid Mech.* 306, 325–352.
- Brent, A. D., Voller, V., Reid, K. J., 1988. Enthalpy-porosity technique for modeling convection-diffusion phase change: Application to the melting of a pure metal. *Numerical Heat Transfer, Part A Applications* 13 (3), 297–318.
- Cardin, P., Olson, P., 1994. Chaotic thermal convection in a rapidly rotating spherical shell: consequences for flow in the outer core. *Physics of the earth and planetary interiors* 82 (3), 235–259.
- Carilli, C. L., Taylor, G. B., 2002. Cluster magnetic fields. *ARAAS* 40, 319–348.
- Cattaneo, F., Emonet, T., Weiss, N., 2003. On the interaction between convection and magnetic fields. *Astrophys. J.* 588 (2), 1183.
- Chandra, M., Verma, M. K., 2013. Flow reversals in turbulent convection via vortex reconnections. *Phys. Rev. Lett.* 110, 114503.
- Chandran, B. D., Dennis, T. J., 2006. Convective stability of galaxy-cluster plasmas. *Astrophys. J.* 642 (1), 140.
- Chandrasekhar, S., 1981. *Hydrodynamic and Hydromagnetic Stability*. Dover Publications, NY.
- Chen, Z. M., Price, W. G., 2006. On the relation between rayleigh–bénard convection and lorenz system. *Chaos, Solitons & Fractals* 28 (2), 571–578.
- Chuzhoy, L., Loeb, A., 2004. Element segregation in giant galaxies and x-ray clusters. *MNRAS* 349, L13–L17.
- Cross, M., Greenside, H., 2009. *Pattern Formation and Dynamics in Nonequilibrium Systems*. Cambridge University Press.
- Getling, A. V., 1997. *Rayleigh–Bénard Convection: Structures and Dynamics*. World Scientific Pub Co Inc.
- Getling, A. V., Brausch, O., 2003. Cellular flow patterns and their evolutionary scenarios in three-dimensional rayleigh–bénard convection. *Phys. Rev. E* 67, 046313.
- Glatzmaier, G. A., Roberts, P. H., 1995. A three-dimensional self-consistent computer simulation of a geomagnetic field reversal. *Nature* 377, 203–209.
- Hartmann, D. L., Moy, L. A., Fu, Q., 2001. Tropical convection and the energy balance at the top of the atmosphere. *J. of Climate* 14, 4495–4511.
- Hollweg, J. V., 1985. Viscosity in a magnetized plasma: Physical interpretation. *J. of Geophysical Research: Space Physics* 90 (A8), 7620–7622.
- Kunz, M., 2011. Dynamical stability of a thermally stratified intracluster medium with anisotropic momentum and heat transport. *MNRAS* 417, 602–616.
- Kunz, M. W., Bogdanović, T., Reynolds, C. S., Stone, J. M., 2012. Buoyancy instabilities in a weakly collisional intracluster medium. *Astrophys. J.* 754 (2), 122.
- Latter, H. N., Kunz, M. W., 2012. The hbi in a quasi-global model of the intracluster medium. *MNRAS* 423, 1964–1972.
- Lesur, G., Ogilvie, G. I., 2010. On the angular momentum transport due to vertical convection in accretion discs. *MNRAS* 404, L64–L68.
- Lorenz, E. N., 1963. Deterministic nonperiodic flow. *J. Atmospheric Sciences* 20, 130–141.
- Marshall, J., Schott, F., 1999. Open-ocean convection: Observations, theory, and models. *Reviews of Geophysics* 37 (1), 1–64.
- McCourt, M., Parrish, I. J., Sharma, P., Quataert, E., 2011. Can conduction induce convection? on the non-linear saturation of buoyancy instabilities in dilute plasmas. *MNRAS* 413, 1295–1310.
- Mckenzie, D. P., Roberts, J. M., Weiss, N. O., 1974. Convection in the earth's mantle: towards a numerical simulation. *J. Fluid Mech* 62, 465–538.
- Morris, S. W., Bodenschatz, E., Cannell, D. S., Ahlers, G., 1993. Spiral defect chaos in large aspect ratio rayleigh–bénard convection. *Phys. Rev. Lett.* 71, 2026–2029.
- Nipoti, C., Posti, L., 2014. On the nature of local instabilities in rotating galactic coronae and cool cores of galaxy clusters. *Astrophys. J.* 792, 21.
- Oliver, G., 2013. Dynamo effects in magnetorotational turbulence with finite thermal diffusivity. *Astrophys. J.* 770 (2), 100.
- Parrish, I. J., McCourt, M., Quataert, E., Sharma, P., 2012. The effects of anisotropic viscosity on turbulence and heat transport in the intracluster medium. *MNRAS* 422, 704–718.
- Parrish, I. J., Quataert, E., 2008. Nonlinear simulations of the heat-flux-driven buoyancy instability and its implications for galaxy clusters. *Astrophys. J. Lett.* 677, L9–L12.
- Parrish, I. J., Quataert, E., Sharma, P., 2009. Anisotropic thermal conduction and the cooling flow problem in galaxy clusters. *Astrophys. J.* 703, 96–108.
- Parrish, I. J., Quataert, E., Sharma, P., 2010. Turbulence in galaxy cluster cores: A key to cluster bimodality? *Astrophys. J. Lett.* 712, L194–L198.
- Parrish, I. J., Stone, J. M., 2005. Nonlinear evolution of the magnetothermal instability in two dimensions. *Astrophys. J.* 633, 334–348.
- Parrish, I. J., Stone, J. M., 2007. Saturation of the magnetothermal instability in three dimensions. *Astrophys. J.* 664, 135–148.
- Parrish, I. J., Stone, J. M., Lemaster, N., 2008. The magnetothermal instability in the intracluster medium. *Astrophys. J.* 688, 905–917.
- Peng, F., Nagai, D., 2009. Effect of helium sedimentation on x-ray measurements of galaxy clusters. *Astrophys. J.* 693, 839–846.
- Pessah, M. E., Chakraborty, S., 2013. The stability of weakly collisional plasmas with thermal and composition gradients. *Astrophys. J.* 764, 13.
- Peterson, J., Fabian, A., 2006. X-ray spectroscopy of cooling clusters. *Phys. Rep.* 427 (1), 1–39.
- Quataert, E., 2008. Buoyancy instabilities in weakly magnetized low-collisionality plasmas. *Astrophys. J.* 673, 758–762.
- Ren, H., Cao, J., Dong, C., Wu, Z., Chu, P. K., 2011. Coupling of kelvin–helmholtz instability and buoyancy instability in a thermally laminar plasma. *Phys. Plasmas* 18 (2), 022110.
- Ren, H., Wu, Z., Cao, J., Chu, P. K., Li, D., 2010. Magnetothermal instability in weakly magnetized plasmas with anisotropic resistivity and viscosity. *Phys. Plasmas* 17 (4), 042117.
- Schekochihin, A. A., Cowley, S. C., Kulsrud, R. M., Hammett, G. W., Sharma, P., 2005. Plasma instabilities and magnetic field growth in clusters of galaxies. *Astrophys. J.* 629, 139–142.
- Schekochihin, A. A., Cowley, S. C., Kulsrud, R. M., Rosin, M. S., Heinemann, T., 2008. Nonlinear growth of firehose and mirror fluctuations in astrophysical plasmas. *Phys. Rev. Lett.* 100 (8), 081301.
- Sharma, P., Hammett, G. W., Quataert, E., Stone, J. M., 2006. Shearing box simulations of the mri in a collisionless plasma. *Astrophys. J.* 637, 952–967.
- Shtykovskiy, P., Gilfanov, M., 2010. Thermal diffusion in the intergalactic medium of clusters of galaxies. *MNRAS* 401, 1360–1368.
- Spitzer, L., 1962. *Physics of Fully Ionized Gases*. Wiley Interscience, New York.
- Stone, J. M., Balbus, S. A., 1996. Angular momentum transport in accretion disks via convection. *Astrophys. J.* 464, 364.
- Zierep, J., 2003. Rayleigh–bénard convection with magnetic field. *Theoretical and Applied Mechanics*, 23–40.